

# Molecular Organization of Gemini Surfactants in Cylindrical Micelles: An Infrared Dichroism Spectroscopy and Molecular Dynamics Study

Reiko Oda,<sup>\*,†</sup> Michel Laguerre,<sup>†</sup> Ivan Huc,<sup>†</sup> and Bernard Desbat<sup>‡</sup>

*Institut Européen de Chimie et Biologie, 16 av. Pey Berland, 33607 Pessac Cedex, France, and Laboratoire de Physico-Chimie Moléculaire, 351 cours de la libération, 33405 Talence, France*

*Received June 10, 2002. In Final Form: September 17, 2002*

The organization of cationic dimeric (gemini) surfactants assembled in cylindrical micelles was investigated using polarization modulation infrared linear dichroism (PM-IRLD) and molecular dynamics simulations. These molecules consist of two quaternary ammonium amphiphiles connected at the headgroup by an ethylene spacer, resulting in an elongated polar head. PM-IRLD measurements and molecular dynamics simulations indicate that the long axis of the surfactant headgroup may adopt a preferred orientation of ca. 30–50° with respect to the micelle cylinder axis. This may be interpreted as the result of the competition between the charge repulsion between headgroups which favors an orientation of the molecules perpendicular to the cylinder axis (high curvature) and the steric repulsion between hydrophobic tails which favors an orientation of the molecules parallel with the cylinder axis (flat curvature). Experiment and calculation both show a water layer a few angstroms thick with a specific orientation at the micelle interface.

## Introduction

In solution, surfactant molecules assemble to form aggregates with various morphologies (e.g., spherical or cylindrical micelles, vesicles, lamellae, etc.) which exhibit diverse sizes (ranging from nanometers to hundreds of microns) and physical properties (e.g., conductivity, viscosity, opacity, or birefringence). The molecular structure of the surfactants strongly affects their packing and intermolecular interactions and, as a result, the size and properties of their aggregates. But this remains difficult to predict, and the rational design of surfactants to produce assemblies with specific properties is still very limited.

To better correlate surfactant structure and aggregate properties, it is essential to obtain more information on the organization of molecules within the aggregates. However, aggregates of surfactants often have “soft” structures: molecules are poorly organized, primarily due to the fact that the driving force for molecular assembly, the hydrophobic effect, imposes little directional constraint and allows a high degree of conformational freedom. For example, even the smallest defined aggregate structures at equilibrium, spherical micelles, consist of as many as 50–100 surfactant molecules. The molecular conformations and positions in the inner structure of micelles are experimentally difficult to determine given that the objects are too small to be observed by light microscopes and too labile to be studied by scattering techniques. Furthermore, structural characterization is further complicated by numerous factors including temperature, ionic force, and the nature of the solvent. Crystal structures provide some atomic level information, but it does not reflect the overall aggregate fluidity which is critically important in determining their physical properties.

In the present study, we use two powerful techniques to provide insight into the molecular organization of gemini surfactant aggregates. We have studied shear-aligned

cylindrical micelles using polarization modulation infrared linear dichroism (PM-IRLD) and have compared these experimental results to the first molecular dynamics simulation of a cylindrical micelle. The amphiphiles we have investigated are gemini<sup>1</sup> (or dimeric) surfactants consisting of two conventional single-tail surfactants connected covalently at their headgroups. These surfactants show quite unusual phase behaviors and have recently motivated numerous studies.<sup>2</sup> The two subunits and the spacer may be varied independently giving access to more structural variations than for their monomeric counterparts. For example, varying the two chain lengths independently already gives  $n(n + 1)/2$  instead of  $n$  variants for the monomer.<sup>2</sup> The most studied class of gemini amphiphiles are cationic bis-quaternary ammonium surfactants having the formula  $C_sH_{2s}\alpha,\omega-((CH_3)_2N^+C_nH_{2n+1}Br^-)((CH_3)_2N^+C_mH_{2m+1}Br^-)$  and are denoted with  $n-s-m$  notation. For this group of surfactants, the effects of the length and the nature of the spacer chain on the critical micelle concentration (cmc), the molecular areas, the behavior at a water–air interface, and the morphology of their aggregates have been reported.<sup>1,3</sup> The effect of varying the counterions<sup>4</sup> and the physicochemical properties of the equivalent trimers and tetramers have also been reported.<sup>5</sup>

Our group has paid particular attention to dimeric amphiphiles with a two-carbon ethylene spacer ( $n-2-$

(1) Menger, F. M.; Littau, C. A. *J. Am. Chem. Soc.* **1991**, *113*, 1451. Zana, R.; Benrraou, M.; Rueff, R. *Langmuir* **1991**, *7*, 1072.

(2) For reviews see: Rosen, M. J.; Tracy, D. J. *J. Surfactants Deterg.* **1998**, *1*, 547. Menger, F. M.; Keiper, J. *Angew. Chem., Int. Ed.* **2000**, *39*, 1906.

(3) (a) Frindi, M.; Michels, B.; Levy, H.; Zana, R. *Langmuir* **1994**, *10*, 1140. (b) Alami, E.; Levy, H.; Zana, R.; Skoulios, A. *Langmuir* **1993**, *9*, 940. (c) De, S.; Aswal, V. K.; Goyal, P. S.; Bhattacharya, S. *J. Phys. Chem. B* **1998**, *102*, 6152. (d) Kim, T.-S.; Kida, T.; Nakatsuji, Y.; Hirao, T.; Ikeda, I. *J. Am. Oil Chem. Soc.* **1996**, *73*, 907. (e) Rosen, M. J.; Song, L. D. *J. Colloid Interface Sci.* **1996**, *179*, 261.

(4) (a) Oda, R.; Huc, I.; Candau, S. J. *Angew. Chem., Int. Ed.* **1998**, *37*, 2689. (b) Oda, R.; Huc, I.; Schmutz, M.; Candau, S. J.; MacIntosh, F. C. *Nature* **1999**, *399*, 566. (c) Bhattacharya, S.; De, S. *Langmuir* **1999**, *15*, 3400.

(5) In, M.; Bec, V.; Aguerre-Chariol, O.; Zana, R. *Langmuir* **2000**, *16*, 141.

\* To whom correspondence should be addressed. Fax: +33 (0)-557 96 22 26. E-mail: r.oda@iecb-polytechnique.u-bordeaux.fr.

<sup>†</sup> Institut Européen de Chimie et Biologie.

<sup>‡</sup> Laboratoire de Physico-Chimie Moléculaire.

*m*).<sup>4a,b,6</sup> Two important characteristics of these compounds are (i) their anisotropic shape, elongated in the direction of the ethylene connection, which may be linked to their strong tendency to assemble into elongated aggregates such as cylindrical micelles, elongated vesicles, or ribbonlike structures at very low concentrations, even in the absence of salt,<sup>6</sup> and (ii) the very short distance (4.0 Å) between the charges of the headgroup, which contrasts with the equilibrium distance of 8–10 Å which can be deduced from the area per headgroup of about 77 Å<sup>2</sup> measured for dodecyltrimethylammonium bromide (DTAB), the monomeric counterpart of 12–2–12.<sup>7,8</sup> This relatively high local charge density may be responsible for another unusual property of these surfactants, which is the tendency of their bilayers to form stacks leaving little water between rather than forming a normal lamellar phase with suspended membranes following the dilution law.<sup>6</sup>

The purpose of the present study was to assess the organization and packing of *n*–2–*n* surfactants within cylindrical micelles in order to evaluate the consequences of their anisotropic shape and high charge density. Cylindrical micelles are flexible fiberlike structures, a few nanometers in diameter and up to tens of microns in length. When they consist of charged amphiphiles, their persistence length is reported to be of the order of a few hundred angstroms.<sup>9</sup> Beyond a certain concentration, such fibers get entangled and form a three-dimensional network, and the solution becomes highly viscoelastic. Solutions as dilute as a few tens of millimolar may be so viscous that the container can be turned upside down without any observable flow. We decided to focus on these objects because they are formed over a large range of concentrations by *n*–2–*n* surfactants, because they can be oriented when the sample is submitted to a shear force allowing dichroic spectroscopic measurements, and because their macroscopic properties such as their morphology<sup>10</sup> and rheology<sup>11,12</sup> have been thoroughly studied.

## Experimental Section

**Sample Preparation.** Hydrocarbon gemini surfactants, 12–2–12 and 8–2–16, with bromide counterions were synthesized as described previously.<sup>6b</sup> The gemini surfactant with fluorocarbon chains, C<sub>2</sub>H<sub>4</sub>-1,2-((CH<sub>3</sub>)<sub>2</sub>N<sup>+</sup>-C<sub>4</sub>H<sub>8</sub>-C<sub>8</sub>F<sub>17</sub>)<sub>2</sub>, and L-tartrate counterions, which is abbreviated as C<sub>8</sub><sup>F</sup>C<sub>4</sub>-2-C<sub>8</sub><sup>F</sup>C<sub>4</sub> was prepared according to previously reported protocols.<sup>13</sup> To prepare the cylindrical micelle solutions, each surfactant was dispersed in Milli-Q deionized water at given concentrations. The solutions were heated to 50 °C for about 15 min<sup>14</sup> and then stored at 30 °C for a day to allow equilibration.

**PM-IRLD.** The measurements were performed on micellar solutions sandwiched between two ZnSe circular windows

(diameter = 3 cm). One of the two windows could rotate and was connected to a thread, which was pulled along the tangential direction (Figure 2). The thickness of the solution was chosen to be ca. 10 μm in order to avoid saturation by the water absorption band at 1650 cm<sup>-1</sup>.

Dichroic difference spectra with a resolution of 4 cm<sup>-1</sup> were obtained using a Nexus 670 spectrometer with an optical setup described previously,<sup>15</sup> a Hinds ZnSe photoelastic modulator operating at 50 Hz, and a Stanford SR 830 numerical lock-in amplifier with a 0.3 ms time constant. All the spectra presented in this paper have been corrected with the Bessel function which was introduced from the photoelastic modulator.<sup>15</sup>

As shown in Figure 2, the incident IR beam was perpendicular to the circular windows and focused at 0.7 cm away from the center of the window where micelles are aligned by shear. At this position, the solution between the two windows is then submitted to a shear rate of 500–1000 s<sup>-1</sup> which is high enough to ensure the parallel alignment of the cylindrical micelles along the shear.<sup>16</sup> Because the gap between the windows is very small compared to their diameter, smooth rotation was possible only with solutions having a high viscoelasticity, the resulting high normal force ensuring sufficient lubrication.<sup>17</sup> The concentration of each surfactant was chosen so that its viscosity is in the range of 10 Pa s, for example, 160 mM (12–2–12), 640 mM (8–2–16), and 50 mM (C<sub>8</sub><sup>F</sup>C<sub>4</sub>-2-C<sub>8</sub><sup>F</sup>C<sub>4</sub>). The sign of the dichroic difference spectra  $A_h - A_v$ , where  $A_h$  is the horizontal absorption and  $A_v$  is the vertical absorption as defined in Figure 2b, was calibrated by measuring the dichroic band of a stretched hydrocarbon polymer having a known molecular orientation with respect to the laboratory axis. The sensitivity of the PM-IRLD method was high enough to obtain spectra with a sufficient signal-to-noise (S/N) ratio in 10–20 scans.

**Molecular Mechanics.** Single molecules of 12–2–12 and C<sub>8</sub><sup>F</sup>C<sub>4</sub>-2-C<sub>8</sub><sup>F</sup>C<sub>4</sub> were built and minimized (MM3\* force field) on an Octane SGI workstation using Macromodel version 6.5 (Columbia University, New York, Schrödinger Inc.) and exported to the Discover version 2000 module of InsightII (Molecular Simulations Inc.) where a semiempirical charge calculation was performed using MOPAC/MNDO and the charges were partitioned into atom groups.

**Molecular Dynamics.** *General.* The dynamics simulations were carried out in the Discover module of Insight with the all-atom Constant Valence force field (CVFF) on a 4-processor SGI Origin 200 server. A 1.5 fs time step was used with a Leapfrog integration algorithm at constant pressure (1 bar). Three-dimensional periodic boundary conditions were applied, and a spherical group-based cutoff with a radius of 13 Å was used throughout. Analysis was performed with the DeCIPHER and Analysis modules of InsightII, and the calculations of projected angles were performed with in-house Fortran programs.

*Single Molecule Dynamics.* One isolated 12–2–12 molecule with its bromide counterions at random positions was placed at the center of a cubic (40 × 40 × 40 Å<sup>3</sup>) box of water (2082 molecules), and the whole assembly was submitted to a molecular dynamics run at 300 K and constant pressure (1 bar) during 500 ps (final density = 1.013). The same procedure was followed with a single isolated molecule of C<sub>8</sub><sup>F</sup>C<sub>4</sub>-2-C<sub>8</sub><sup>F</sup>C<sub>4</sub> in a box of identical dimensions (2072 water molecules). In this case, the final density was 1.026.

*Construction and Dynamics of a Cylindrical Micelle.* As shown in Figure 1a, twelve 12–2–12 molecules were regularly placed as the spokes of a wheel (30° steps). The N–N vectors of the gemini molecules were initially parallel to the axis of this disk-like assembly. Six of these disks were stacked at 10.5 Å intervals, yielding a cylindrical micelle consisting of 72 amphiphiles and 144 hydrocarbon tails. The N–N vectors were offset by alternatively rotating the disks by 15° (Figure 1b). This arrangement generates a specific surface of ca. 95 Å<sup>2</sup> per molecule.<sup>6</sup> The 144

(6) (a) Oda, R.; Huc, I.; Homo, J.-C.; Heinrich, B.; Schmutz, M.; Candau, S. *J. Langmuir* **1999**, *15*, 2384. (b) Oda, R.; Huc, I.; Candau, S. *J. Chem. Commun.* **1997**, 2105.

(7) Zana, R. *J. Colloid Interface Sci.* **1980**, *78* (2), 330.

(8) Bales, B.; Zana, R. *J. Phys. Chem. B* **2001**, *106* (8), 1926.

(9) Marignan, J. A.; Bassereau, P.; Porte, G.; May, R. P. *J. Phys.: Condens. Matter* **2** **1989**, *50*, 3553.

(10) (a) Zana, R.; Talmon, Y. *Nature* **1993**, *362*, 228. (b) Bernheim-Groswasser, A.; Zana, R.; Talmon, Y. *J. Phys. Chem. B* **2000**, *17*, 4005.

(11) Kern, F.; Lequeux, F.; Zana, R.; Candau, S. *J. Langmuir* **1994**, *10*, 1714.

(12) (a) Cates, M. E.; Candau, S. *J. Phys.: Condens. Matter* **1990**, *2*, 6869. (b) Rehage, H.; Hoffmann, H. *Mol. Phys.* **1991**, *74*, 933. (c) Hoffmann, H. In *Structure and Flow in Surfactant Solutions*; Herb, C., Prudhomme, R., Eds.; ACS Symposium Series, No. 578; American Chemical Society: Washington, DC, 1994; Chapter 1.

(13) Oda, R.; Huc, I.; Danino, D.; Talmon, Y. *Langmuir* **2000**, *16*, 9759.

(14) Cylindrical micelles are structures at thermodynamic equilibrium. In principle, the surfactants dissolve without heating. However, since dissolution is often very slow, the mixtures are heated at a temperature which do not result in surfactant degradation.

(15) Buffeteau, T.; Desbat, B.; Bokobza, L. *Polymer* **1995**, *36*, 4339.

(16) Berret, J.-F.; Roux, D. C.; Porte, G.; Lindner, P. *Europhys. Lett.* **1994**, *25*, 521.

(17) Due to its viscoelastic behavior, the solution of entangled cylindrical micelles exhibits a positive normal force difference in the direction perpendicular to the shear direction, as is the case in many viscoelastic fluids. This normal force is due to the strong orientation of the micelles parallel to the velocity direction.

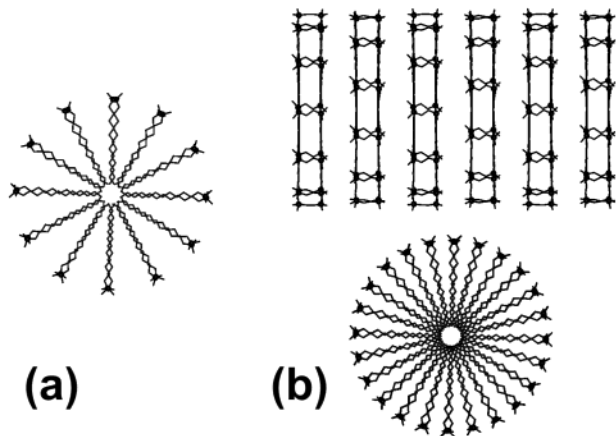


**Figure 1.** Construction of a cylindrical micelle.

bromide counterions were randomly placed around the micelle, and this assembly was surrounded by 5328 water molecules in a  $63 \times 60 \times 60 \text{ \AA}^3$  box for a total of 23 180 atoms. The cylinder axis lies along the Ox axis (63 Å) of the box. After a careful minimization, the whole system was submitted to a molecular dynamics run at 300 K at constant volume for 500 ps and then at constant pressure for a further 1.5 ns. On the 4-processor SGI Origin 200 servers, the calculation lasted 15 days per ns.

## Results

### Conception of the Setup and Theoretical Model.

PM-IRLD allows the quantitative determination of the orientation of molecules with respect to a fixed laboratory axis. This technique has been successfully used to study light-induced orientation of azopolymers<sup>18</sup> and the orientation and relaxation of polymer blends.<sup>19</sup> Here, we apply this technique to assess the organization of amphiphiles within cylindrical micelles aligned by shear. The setup described in Figure 2a shows the micelles aligned between two windows perpendicular to the incident beam. The dichroic signal corresponds to the difference between the absorption of light polarized "horizontally" (which was assumed to be parallel to the axis of the micelle cylinders) and the absorption of light polarized "vertically" (which was assumed to be perpendicular to the axis of the micelles (Figure 2b).

To relate the observed dichroic signals to the orientation of the amphiphiles in the cylindrical micelles, we constructed the following model. For a given oscillating dipole, the absorbance is proportional to the square of the scalar product between the dipole moment and the external electric field. If the dipole moment is at an angle  $\phi$  from the electric field, it can be written as

$$A_b \propto (\vec{\mu} \cdot \vec{E})^2 = \left(\frac{\partial \mu}{\partial Q}\right)^2 E^2 \cos^2 \phi \quad (1)$$

If the oscillating dipole has a completely isotropic distribution, identical absorptions are expected for both polarized directions of the incident beam, and no dichroic signal should result. In the present configuration, we consider a dipole on a surfactant molecule of the oriented cylinder. We thus assumed that this dipole has a cylindrical symmetry (see Figure 2). We define the angle between the dipole moment and the cylinder axis as  $\alpha$ . To calculate the absorption of the oscillating dipole in the horizontal and vertical directions, we should perform the integral of  $(\vec{\mu} \cdot \vec{E})^2$  over the cylinder. The term  $(\partial \mu / \partial Q)$  of eq 1 is a

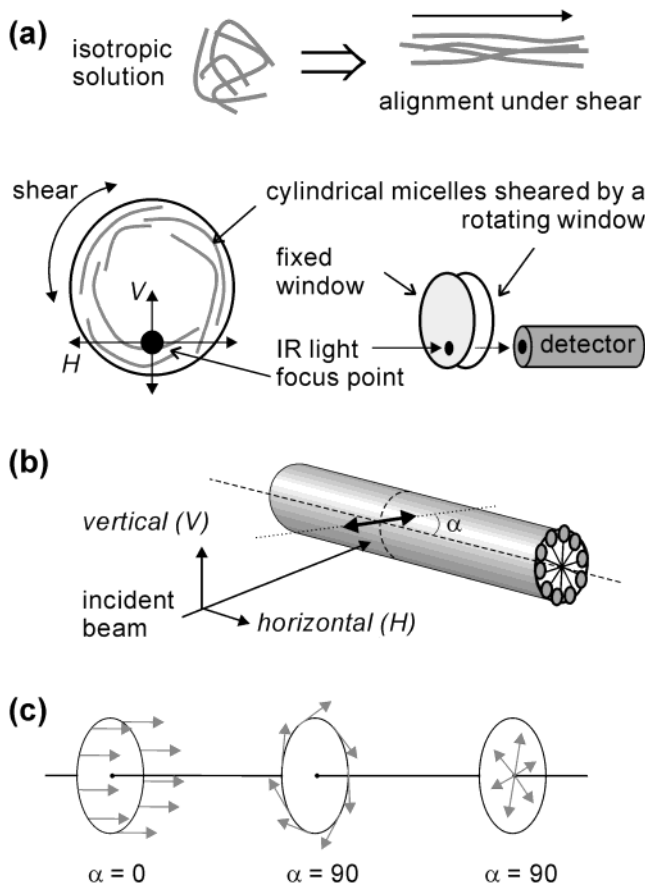


**Figure 2.** (a) Experimental setup for the PM-IRLD. Micelles are aligned by shear perpendicularly to the incident beam. (b) Definition of the vertical and horizontal polarization of IR light with respect to the micelle axis and of the angle,  $\alpha$ , between an oscillating dipole and the micelle axis. (c) Cylindrical distribution of various dipoles on the micelle for  $\alpha = 0^\circ$  and  $\alpha = 90^\circ$ .

constant which depends on the vibration in the molecules. Hereafter,  $(\partial \mu / \partial Q)$  will be abbreviated as  $M$ ; the horizontal absorption  $A_h$  and the vertical absorption  $A_v$  can be written

$$A_h \propto \int_0^{2\pi} d\theta (\vec{\mu} \cdot \vec{E}_h)^2 = M^2 E^2 \cos^2 \alpha \int_0^{2\pi} d\theta = 2\pi M^2 E^2 \cos^2 \alpha$$

$$A_v \propto \int_0^{2\pi} d\theta (\vec{\mu} \cdot \vec{E}_v)^2 = M^2 E^2 \int_0^{2\pi} d\theta (\cos^2 \theta \sin^2 \alpha) = \pi M^2 E^2 \sin^2 \alpha$$

And the dichroic signal is

$$A_h - A_v = M^2 E^2 (2\pi \cos^2 \alpha - \pi \sin^2 \alpha) = \pi M^2 E^2 (3 \cos^2 \alpha - 1) \quad (2)$$

This calculation allows one to determine the dichroic difference between a privileged direction and a transition moment which is at a given angle from this direction.<sup>20</sup> Note that even if  $\alpha$  has a random distribution from  $0^\circ$  to  $360^\circ$ , the average value of  $\cos^2 \alpha$  is  $1/2$ , and the average value of  $A_h - A_v$  is  $\pi M^2 E^2 / 2$ ; that is, a positive dichroic signal is expected. This is the case for a dipole perpendicular to the alkyl chain of a surfactant molecule, when this molecule, oriented radially in the micelle, rotates freely about itself. The fact that the dipoles have cylindrical

(18) Buffeteau, T.; Pérolet, M. *Appl. Spectrosc.* **1996**, *50*, 948.

(19) Pérolet, M.; Pellerin, C.; Prud'homme, R. E.; Buffeteau, T. *Vib. Spectrosc.* **1998**, *18*, 103.

(20) Siesler, H. W.; Holland-Moritz, K. *IR and Raman Spectroscopy of Polymers*; Marcel Dekker: New York, 1980; Chapter 4.3, p 238.

symmetry results in a positive dichroic signal. On the other hand, if  $\alpha$  adopts a fixed average value which indicates a particular orientation of the surfactant, eq 2 shows that a positive dichroic signal is expected when  $|\alpha| < 54.7^\circ$ , for example, when the dipole is parallel to the cylinder axis (Figure 2c). A negative dichroic signal is expected when  $54.7^\circ < |\alpha| < 125.3^\circ$ , when the dipole is oriented radially, or when the dipole is tangent and perpendicular to the cylinder (Figure 2c). No dichroic signal is expected when  $\alpha = 54.7^\circ$ .

This analysis can be extended further for the particular case of  $\text{CH}_2$  or  $\text{CF}_2$  groups in the hydrophobic tails of the surfactants, which give rise to distinct symmetric and antisymmetric vibrations perpendicular to each other. If we define the symmetrical vibration of  $\text{CH}_2$  (or  $\text{F}_2$ ) groups to be at an angle  $\alpha$  from the cylinder axis,

$$(A_h - A_v)_{\text{sym}} = \pi M_{\text{sym}}^2 E^2 (3 \cos^2 \alpha - 1)$$

$$(A_h - A_v)_{\text{antisym}} = \pi M_{\text{antisym}}^2 E^2 (3 \cos^2(\alpha + 90) - 1) = \pi M_{\text{antisym}}^2 E^2 (3 \sin^2 \alpha - 1)$$

The ratio between the expected dichroic signals of these two vibrations is thus

$$\frac{(A_h - A_v)_{\text{sym}}}{(A_h - A_v)_{\text{antisym}}} = \frac{M_{\text{sym}}^2 E^2 (3 \cos^2 \alpha - 1)}{M_{\text{antisym}}^2 E^2 (3 \sin^2 \alpha - 1)}$$

$$r \equiv \frac{(A_h - A_v)_{\text{sym}}}{(A_h - A_v)_{\text{antisym}}} \frac{M_{\text{antisym}}^2 E^2}{M_{\text{sym}}^2 E^2} = \frac{(3 \cos^2 \alpha - 1)}{(3 \sin^2 \alpha - 1)} \quad (3)$$

Since  $M_{\text{antisym}}^2 E^2 / M_{\text{sym}}^2 E^2$  can be measured from the bulk absorption spectra, this equation allows one, in principle, to calculate  $\alpha$  (defined above as the direction of the symmetric vibration).

**IR Measurements.** IR measurements were performed on micellar solutions of surfactants 12-2-12 and 8-2-16 with bromide counterions and of fluorinated surfactant  $\text{C}_8^{\text{F}}\text{C}_4-2-\text{C}_8^{\text{F}}\text{C}_4$  with L-tartrate counterions.<sup>21</sup> The solutions of 12-2-12 and 8-2-16 have similar aggregation behaviors, and the IR-LD spectra of 12-2-12 and 8-2-16 were essentially the same. However, the domain of existence of cylindrical micelles is shifted to higher concentrations for 8-2-16. Measurements with this surfactant thus feature a better signal-to-noise ratio.

Bulk absorption spectra of nonoriented solutions were first measured to assign the various bands to the corresponding vibrators. The spectrum of a micellar solution of 8-2-16 at 640 mM is shown in Figure 3a. The spectrum of 12-2-12 at 160 mM is essentially similar (not shown). Both spectra are dominated by the water absorption bands at  $\sim 3400$  and  $\sim 1650$   $\text{cm}^{-1}$ . The gemini amphiphilic molecules are characterized by the bending and stretching vibrations of the hydrocarbon chain  $\text{CH}_2$  groups at 1450  $\text{cm}^{-1}$  ( $\delta$ ), 2850  $\text{cm}^{-1}$  ( $\nu_s$ ), and 2920  $\text{cm}^{-1}$  ( $\nu_a$ ). There are also other characteristic absorption bands due to the methyl groups of the polar heads at 2950 and 1490  $\text{cm}^{-1}$ . According to powder absorption spectra (not shown), a peak is expected at 900  $\text{cm}^{-1}$  which can be attributed to  $\nu$  C-N from quaternary ammoniums. However, in the gel bulk spectra, this peak is buried under the large absorption of water.

(21) With bromide counterions,  $\text{C}_8^{\text{F}}\text{C}_4-2-\text{C}_8^{\text{F}}\text{C}_4$  forms stable vesicles, but with tartrate, this surfactant assembles into cylindrical micelles.

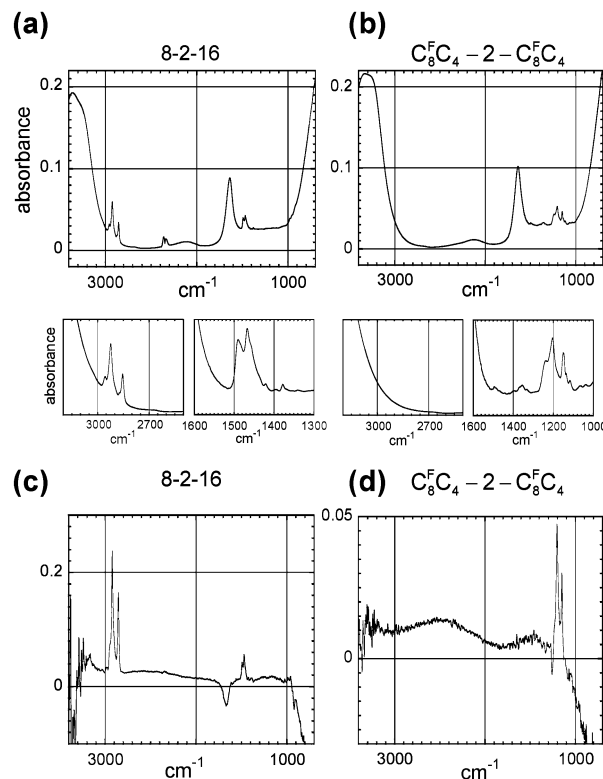


**Figure 3.** IR absorption spectra (top) of a 640 mM micellar solution of 8-2-16 (a) and of a 50 mM solution of  $\text{C}_8^{\text{F}}\text{C}_4-2-\text{C}_8^{\text{F}}\text{C}_4$  (b); PM-IRLD dichroic difference spectra (bottom) of the same solutions under shear ((c) and (d), respectively).

The IR absorption spectrum of a 50 mM micellar solution of  $\text{C}_8^{\text{F}}\text{C}_4-2-\text{C}_8^{\text{F}}\text{C}_4$ -tartrate (Figure 3b) shows the stretching vibrational bands of the fluorocarbon  $\text{CF}_2$  at 1210 and 1150  $\text{cm}^{-1}$ , the bending vibration bands of the methyl groups of the polar heads at 1490  $\text{cm}^{-1}$  ( $\delta_a$ ), and the stretching vibration bands of the  $\text{CF}_3$  groups at the end of the chains at 1240  $\text{cm}^{-1}$  ( $\nu_a$ ) and 1130  $\text{cm}^{-1}$  ( $\nu_s$ ). Peaks at 1360  $\text{cm}^{-1}$  can be assigned to the symmetric stretching vibration ( $\nu_s$ ) of the  $\text{COO}^-$  groups of tartrate anions, and the two peaks at around 1050  $\text{cm}^{-1}$  can be assigned to the  $\nu$  C-O.

The dichroic difference spectrum of a solution of 8-2-16 under shear (Figure 3c) shows several clear bands. As for the bulk absorption spectra, the PM-IRLD spectra recorded for 12-2-12 at 160 mM are essentially similar to the 8-2-16 spectrum. The dominant signals are the antisymmetric and symmetric positive vibration bands of  $\text{CH}_2$  at 2920 and 2850  $\text{cm}^{-1}$  and the bending band of  $\text{CH}_2$  at 1450  $\text{cm}^{-1}$ . Other positive signals due to the methyl groups of the polar heads are present at 1490 and 2950  $\text{cm}^{-1}$ . Another peak related to the headgroups is the negative signal of the C-N  $\nu_a$  vibration at around 900  $\text{cm}^{-1}$ . A quite striking signal is the negative band at  $\sim 1650$   $\text{cm}^{-1}$ , due to the bending of water molecules.

The dichroic difference spectrum of the fluorinated gemini micellar solution under shear also shows clear dichroism (Figure 3d). Fluorinated chains give rise to positive symmetric and antisymmetric bands at 1150 and 1200  $\text{cm}^{-1}$ , respectively. A negative band at 1240  $\text{cm}^{-1}$  can be attributed to the stretching vibration of the  $\text{CF}_3$  groups ( $\nu_a$ ). A weak negative component from tartrate vibrations appears at around 1340  $\text{cm}^{-1}$ . Compared to hydrogenated gemini solutions, interesting differences can be remarked: the absence of signals due to water molecules or hydrocarbon groups even though 4 of the 12 carbons

in the hydrophobic chains of  $C_8^F C_4-2-C_8^F C_4$  are hydrogenated.

**Molecular Modeling.** Molecular dynamics simulations of isolated gemini surfactant molecules and of a cylindrical micelle were performed to obtain a detailed picture of the position of the amphiphiles in the micelles and its evolution with time.

*Single Amphiphilic Molecules.* The dynamic simulation of isolated amphiphilic molecules (12-2-12 and  $C_8^F C_4-2-C_8^F C_4$ ) allowed us to calibrate the force field and the molecular dynamics procedure used throughout this study (see Experimental Section). The gauche conformer content of the two gemini surfactants was monitored during these experiments. Considering 20 dihedral angles for the two alkyl chains of a surfactant molecule and not taking into account rotations about the bonds of the ethylene spacer or those adjacent to the nitrogens,<sup>22</sup> the average number of gauche conformations for 12-2-12 is 3.7, slightly less than 2 gauche conformations per alkyl chain. In contrast, the fluorinated derivative shows no gauche conformations.

The diffusion of water molecules during the simulation was also followed. A diffusion coefficient  $D = 3.71 \pm 0.02 \times 10^{-5} \text{ cm}^2/\text{s}$  was obtained with the Insight II computing package, using Einstein's equation:  $1/6$  of the slope of the mean square displacement versus time.<sup>23,24</sup> This value is close to the diffusion coefficient of free water<sup>25</sup> and shows that a single surfactant molecule in a 40 Å cubic box does not significantly affect diffusion.

*Cylindrical Micelle.* After a 2 ns molecular dynamics simulation at constant pressure, the final micelle appears as a smooth cylinder (Figure 4). As shown in Figure 5c, the gyration radius (defined as the radius of a cylinder having the same gyration moment), not including bromides and penetrating water molecules, fluctuates during the first nanosecond before reaching a very stable value (fluctuations below 0.1 Å). On average, during the last 100 ps the gyration radius is estimated at  $24.08 \pm 0.019$  Å. In the following, the micelle is described in terms of the radial distribution of atoms, the conformations of the amphiphiles, and the orientations of various groups.

The cylindrical radial diffusion function (RDF) of representative atoms such as nitrogens, bromides, and oxygens is reported in Figure 5a,b. From Figure 5b, the actual radius of the micelle including bromides is estimated to be about 25 Å. About 70% of the nitrogens and 65% of the bromides are found between 15 and 21 Å from the axis of the cylinder. Moreover, a closer examination of the cumulative number graph (Figure 5a) reveals an almost identical repartition of the positively and negatively charged groups. Tubes excluding 25% of these atoms in their interior and 25% in their exterior (thus overlapping with the central 50%) have a radius of  $19.0 \pm 2.7$  Å for nitrogens and of  $19.0 \pm 3.3$  Å for bromides. This is in good

(22) For both steric and electrostatic reasons, gauche conformations about the central C-C spacer bond are unlikely. On the other hand, bonds adjacent to the nitrogens always have gauche conformations.

(23) Allen, M. P.; Tildesley, D. J. *Computer simulations of liquids*; Clarendon Press: Oxford, 1989.

(24) This equation has been derived for isotropic motions and is valid provided that the correlation time for a given diffusive motion is much smaller than the time frame of the entire molecular dynamics calculation. In the present case, we are well within the limits of validity.

(25) In fact, this value is higher than the experimental value at 300 K ( $2.3 \times 10^{-5} \text{ cm}^2/\text{s}$ ). However, all models of water (including TIP3P) are too diffusive (Jorgensen, W. L.; Chandrasekhar, J.; Madura, J. D.; Impey, R.; Klein, M. L. *J. Chem. Phys.* **1983**, *79*, 926). For example, the correct  $D$  parameter for water at 300 K can be found with a TIP3P simulation performed at 273 K. In the present context, we use  $D = 3.71 \times 10^{-5} \text{ cm}^2/\text{s}$  for water that diffuses freely and compare it to the diffusion of restrained water molecules calculated under the same condition.

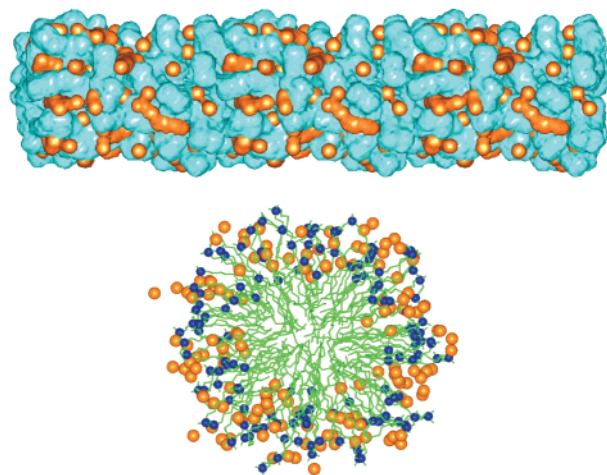


**Figure 4.** The structure of a cylindrical micelle after a 2 ns molecular dynamics simulation. Top: Micelle built from 3 units of the simulation box along the Ox axis (boxes -1 to +1) showing the solvent accessibility surface of the surfactants (blue) and of the bromide ions (orange). Bottom: View down the axis of the cylinder. Carbons are shown as green sticks. Nitrogen atoms and bromide ions are shown as blue and orange Corey-Pauling-Koltun (CPK) spheres (radius = 0.5), respectively. Hydrogens are omitted for clarity.

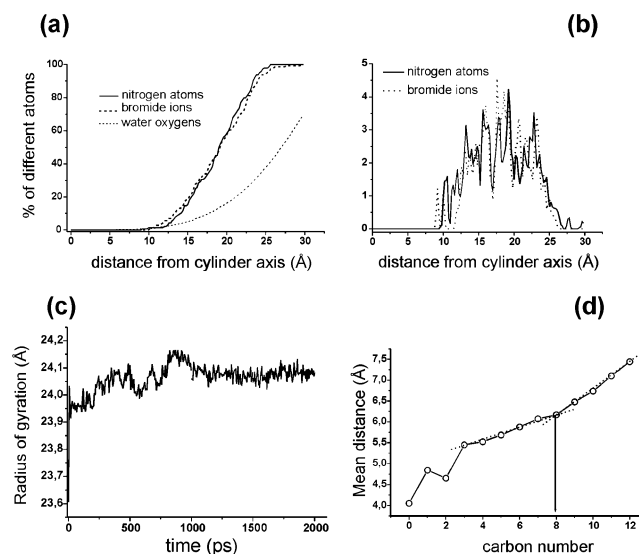


**Figure 5.** Structures of the micelle and of the amphiphiles according to molecular dynamics simulations: (a) percentage of included N, Br, and O atoms from the cylinder axis averaged over the last 100 ps of the simulation; (b) radial distribution functions of N and Br counted at intervals of 0.2 Å; (c) radius of gyration of the cylindrical micelle vs time; (d) intramolecular distances between equivalent carbons of the two alkyl chains averaged during the last 100 ps of the simulation over the 72 amphiphiles of the simulation box. Rank 0 gives the N...N distance as a reference.

agreement with the average location of bromide ions determined experimentally using X-ray diffraction at  $18.3 \pm 2$  Å from the micelle axis.<sup>26</sup> This confirms that the micelle simulated during 2 ns is almost equilibrated and very close to the experimentally determined structure.

The interior of the micelle appears "dry" with only a few water molecules occasionally wandering in as deep as  $\sim 4$  Å from the axis. As shown in Figure 5a, the amount of water begins to be significant beyond 12 Å from the

(26) Weber, V. Ph.D. Thesis, University of Louis Pasteur, Strasbourg, France, 2001.

axis, where one can find the first charged atoms. The diffusion coefficient  $D$  of water molecules in the simulation box in the presence of the micelle was calculated to be  $2.07 \times 10^{-5} \text{ cm}^2/\text{s}$ . This can be interpreted as immobilization of 45% of the water molecules and free diffusion of the remaining water molecules (recall that the diffusion coefficient of free water was determined to be  $3.71 \times 10^{-5} \text{ cm}^2/\text{s}$ ). Figure 5a shows that 45% of the water is found within  $26.3 \text{ \AA}$  of the micelle axis in the vicinity of charged atoms. The layer of bound water can be estimated to be  $5\text{--}7 \text{ \AA}$  thick.

The conformation of the amphiphiles in the micelles can be described by the content of gauche conformations and by the distance between equivalent carbons on the two hydrocarbon tails of the same molecule. This distance reveals that the tails diverge from the headgroup (Figure 5d). From  $4 \text{ \AA}$  between the nitrogens, the distance between equivalent carbons rapidly increases to  $5.45 \text{ \AA}$  for  $C_3$  ( $C_1$  is the first carbon from the ammonium). It increases further at the rate of ca.  $0.14 \text{ \AA}/\text{bond}$  from  $C_3$  to  $C_8$  and then at a rate of  $0.30 \text{ \AA}/\text{bond}$  from  $C_8$  to  $C_{12}$ .

The averaged gauche conformer content of the 12–2–12 molecules was followed during the whole simulation, and it stabilized to ca.  $3.74 \pm 0.13$  during the last 500 ps (about 2 gauche conformations per alkyl chain). This is the same as the value found for an isolated molecule (see above), suggesting that a gemini does not experience any particular conformational constraint when in a micellar environment. The distribution of gauche conformations along the chains reveals that most rotations have an average gauche ratio of  $12 \pm 4\%$ . Two noticeable exceptions are conformations about the  $C_3\text{--}C_4$  bonds, which are 30% gauche, and conformations about the  $C_1\text{--}C_2$  bonds, which are only 2% gauche. This low gauche content at the  $C_1\text{--}C_2$  bond is related to the plateau of the interchain distance observed for  $C_1$  and  $C_2$  (Figure 5d).

Because of its significance for the interpretation of the PM-IRLD spectra, the positioning of the surfactants in the micelle was followed by measuring the orientation of the headgroups and the  $\text{CH}_2$  vibrators of the alkyl chains with respect to the micelle axis. The orientation of water molecules was also monitored.

For the headgroups, we considered both the N–N vector and its projection on the plane tangent to the cylinder intersecting N–N at its midpoint. The angle between the projection and the micelle axis defines the azimuth of the surfactant, and the angle between the projection and the vector N–N defines the inclination of the surfactant. In the initial micelle, all azimuth and inclination angles are equal to  $0^\circ$ . During the initial energy minimization, the azimuth angle changes rapidly to give the distribution shown in Figure 6 ( $t = 0 \text{ ns}$ ), with a maximum at  $20^\circ$  and another smaller peak at  $-20^\circ$ . During the first 0.5 ns of the dynamic simulation, it slowly increases and reaches a value of ca.  $35^\circ$  that remains stable during the last 1.5 ns (Figure 6). A very similar phenomenon is observed for the inclination angle. It first rapidly increases to about  $16^\circ$  during the minimization and then slowly increases during the dynamic simulation to reach a value of  $19^\circ \pm 0.3$  that remains stable during the last 1 ns.

Figure 7 shows the distributions of angles between the micelle axis and the H–H vectors of the  $\text{CH}_2$  groups of the alkyl chains, for each carbon from  $C_1$  to  $C_{11}$ . This vector corresponds to the direction of the antisymmetric vibration. It can clearly be seen that at any position except  $C_{11}$ , very few H–H vectors are either parallel ( $0^\circ$ ) or perpendicular ( $90^\circ$ ) to the cylinder axis. Most vibrators have a preferred orientation between  $30^\circ$  and  $60^\circ$ . We note that this orientation increases more or less regularly from  $C_2$

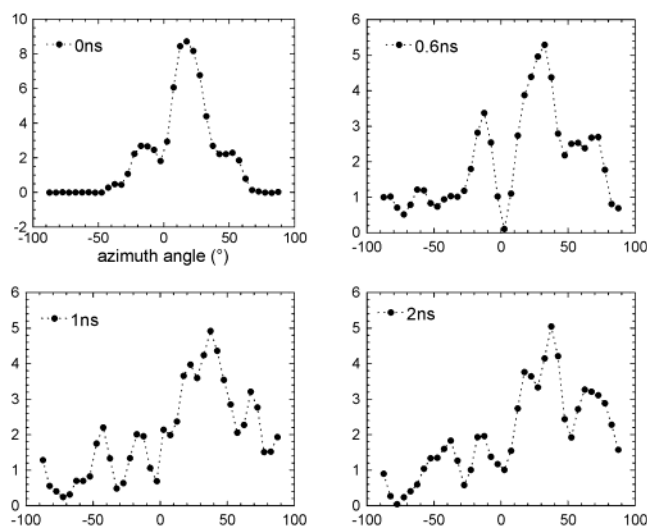


**Figure 6.** Temporal variation of the N–N azimuth angle (see the text for a definition).

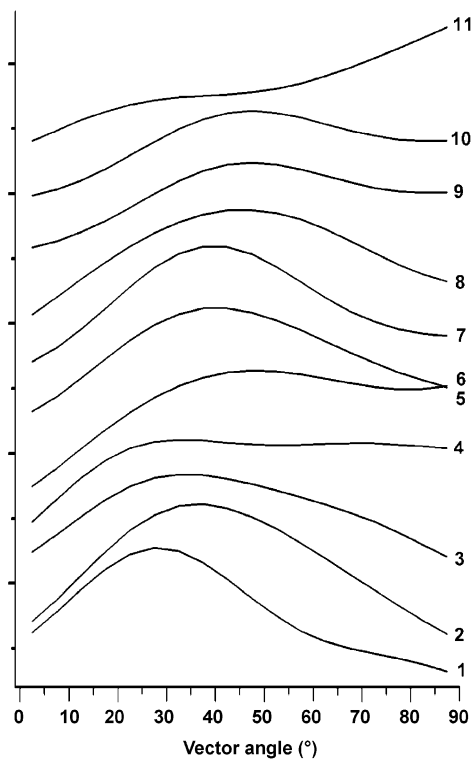


**Figure 7.** Distribution of the angles between H–H vectors and the micelle axis of alkyl chains for each carbon from  $C_1$  to  $C_{11}$ .

( $30^\circ$ ) to  $C_{10}$  ( $45^\circ$ ), which suggests a slight tendency of the chain to twist.  $C_{11}$  has a very different distribution, which can probably be attributed to its position almost at the end of the fluid chain.

The orientation of the water molecules was estimated by calculating the angle between their dipole moments (which gives the direction of the symmetric vibration) and a plane perpendicular to the axis of the cylinder for all 5328 water molecules in the box after 2 ns of simulation. These angles were counted from  $0$  to  $90^\circ$  using  $1^\circ$  intervals, which gives the angular distribution shown in Figure 8. In a random distribution, all angles have the same probability, and a horizontal line would be expected. Figure 9 shows a very strong deviation from a random distribution, with a clear dominance of low angles. From the

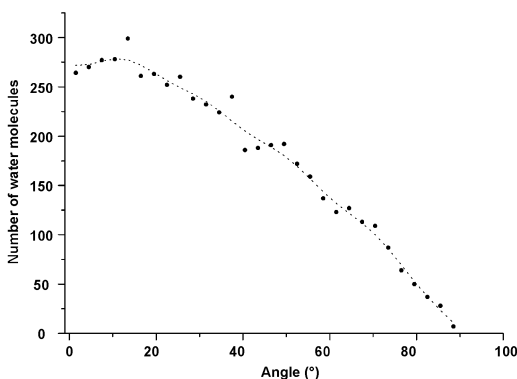


**Figure 8.** Distribution of the angles between the water dipole moments and a plane perpendicular to the axis of the cylinder. Molecules are counted for each angle at  $1^\circ$  successive intervals.

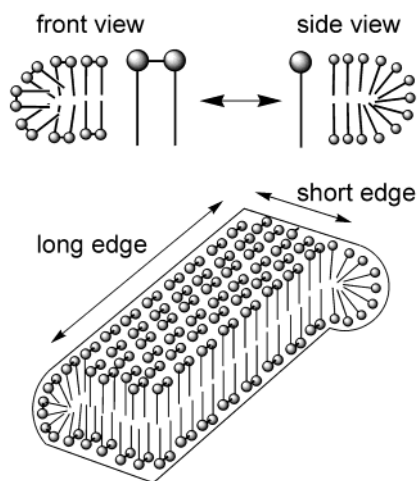


**Figure 9.** Dissymmetric molecular shape of gemini amphiphiles and the difference in line tension in the presence of nematic ordering.

integration of the curve, we find that 50% (instead of 31%) of all dipoles are found at angles below  $28^\circ$ . In other words, 72% (instead of 50%) of the molecules are oriented at angles below  $45^\circ$ .

### Analysis and Discussion

The surfactants studied here are particularly prone to forming cylindrical micelles as well as other elongated aggregates such as flat or twisted ribbons and tubules, even at low concentrations.<sup>4,6,10</sup> It has been hypothesized that this ability to form anisotropic aggregates may originate from the anisotropic shapes of the molecules themselves. As shown in Figure 9, steric hindrance allows one to expect that forming an edge in an aggregate may be more difficult along the N–N axis of the gemini amphiphile than in the direction perpendicular to the N–N axis. Thus, a preferential orientation of gemini surfactants in the aggregates may lead to different line tensions along perpendicular directions, resulting in the formation of elongated aggregates having both long and short edges, such as ribbons or cylindrical micelles. Theoretical models based solely on steric interaction have been reported.<sup>27</sup> In reality, however, one may expect charge repulsions to also play a vital role in gemini surfactant aggregation. In the following discussion, the results presented above are subjected to this model.

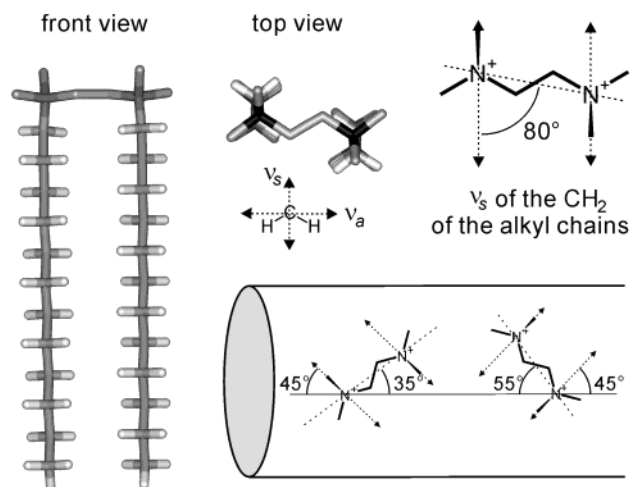


**Figure 10.** Energy-minimized structure of a gemini molecule (hydrogens of the headgroup are omitted for clarity) and the two positions of the headgroups on a cylindrical micelle orienting the symmetric  $\nu_s$  of the alkyl chains at  $45^\circ$  with respect to the cylinder axis.

The model we have developed to interpret the IR spectroscopic data shows that the dichroic signal under the assumption of cylindrical symmetry has an angular dependence as shown in eq 2. This means that while negative PM-IRLD signals unambiguously demonstrate a preferred orientation of the corresponding vibrators ( $54.7^\circ < |\alpha| < 125.3^\circ$ ), the positive signals remain ambiguous as they may arise either from a preferred ( $|\alpha| < 54.7^\circ$ ) or from a random orientation. On the other hand, the analysis of the results from the molecular dynamics simulations decidedly reveals an anisotropic organization of the gemini surfactants with respect to the micellar axis. The orientations of the N–N vectors of the headgroups rapidly change from their initial values to reach a stable state and remain at this value for the remainder of the simulation.

If we assume a nonrandom orientation of the alkyl chains, the model presented above can be developed to calculate the orientation  $\alpha$  of the symmetric  $\text{CH}_2$  vibrator from the relative absorption intensities of the symmetric and antisymmetric vibrations and from the relative intensities of their dichroic signals (eq 3). This analysis yields values of  $\alpha = 47.0^\circ$  for 12–2–12,  $\alpha = 45.8^\circ$  for 8–2–16, and  $\alpha = 44.5^\circ$  for  $\text{C}_8^{\text{F}}\text{C}_4\text{--}2\text{--}\text{C}_8^{\text{F}}\text{C}_4$ . Two other similar gemini surfactants with different hydrocarbon chain lengths (data not shown) yielded values of  $45.2^\circ$  and  $45.5^\circ$ . In all cases, dichroic signals are positive for both symmetric and antisymmetric vibrations, which implies that  $|\alpha| < 54.7^\circ$  and  $|\alpha + 90| < 54.7^\circ$  and is consistent with the calculated values  $35.3^\circ < |\alpha| < 54.7^\circ$ . These values of  $\alpha$  of ca.  $45^\circ$  can be compared with the molecular modeling results which give a preferred orientation of the H–H vector at  $30\text{--}45^\circ$  with respect to the cylinder axis (Figure 7), implying  $\alpha$  to be  $45\text{--}60^\circ$  for the symmetric  $\text{CH}_2$  vibrations.

From the orientation of the alkyl chains, we can now deduce the orientation of the polar head (N–N vector). In the energy-minimized conformation of a gemini surfactant shown in Figure 10, ammonium groups are in the anti conformation about the central spacer bond. Both alkyl chains lie parallel, and their direction is perpendicular to the N–C–C–N spacer plane,<sup>22</sup> which is therefore roughly parallel to the surface of the cylindrical micelle. For such conformations, the angle between the  $\text{CH}_2$  (or  $\text{CF}_2$ ) symmetric vibration and the N–N direction can be

(27) (a) Fournier, J. B.; Galatola, P. *J. Phys. II France* **1997**, *7*, 1509. (b) Fournier, J. B.; Galatola, P. *Braz. J. Phys.* **1998**, *28*, 329.

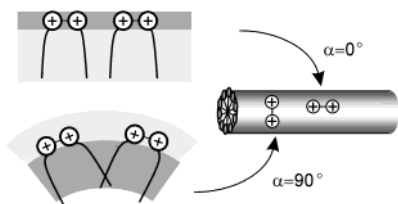


**Figure 11.** Steric hindrance and charge repulsion may be in competition to determine the azimuth angle of gemini molecules at the surface of cylindrical micelles.

calculated to be ca.  $80^\circ$ . The PM-IRLD data indicate that the direction of the symmetric vibration is oriented at  $\sim|45^\circ|$  with respect to the axis of a cylindrical micelle (and the antisymmetric vibration as well, since they are perpendicular to each other). Thus, two positions for the gemini surfactants are possible ( $+45^\circ$  and  $-45^\circ$ ) in which the N–N vector is oriented at  $35^\circ$  or  $55^\circ$  from the cylinder axis (Figure 10). This is also in agreement with the molecular modeling results which show that the N–N direction has a preferred orientation at around  $\pm 30\text{--}50^\circ$  from the micellar axis (Figure 6).

The fact that very few molecules are oriented with N–N at  $90^\circ$  (Figure 6) can be understood as a consequence of steric hindrance. The dynamics simulations indicate that the N–N distance of the gemini is about 4 Å, while the hydrocarbon chains have mean distances of more than 5 Å. The molecules thus have the shape of long rectangles which are easier to pack radially with the N–N axis parallel to the micelle rather than perpendicular to the micelle (Figure 9).

The reason very few molecules are oriented with N–N at  $0^\circ$  (Figure 6) is more subtle, since this orientation would be the most favorable from the point of view of packing. We suggest that this tilt of the N–N direction is due to the charge repulsions associated with the high charge density at the gemini headgroup which results from the very short distance between the ammonium groups. As shown in Figure 11, the least favorable orientation in terms of steric effects ( $\alpha = 90^\circ$ ) also corresponds to the largest separation between the charged headgroups. Conversely, when  $\alpha = 0^\circ$ , the charges are not well separated.

Another aspect of the charge constraint on the orientation of the molecules concerns the inclination angle of the N–N vector with respect to the surface of the micellar cylinder. Molecular modeling gives a preferred inclination of  $19^\circ$ , indicating that the N–N plane of the headgroups is not tangential to the surface of the micelle. Again, this may be interpreted as spreading the charges away from each other. We found similar results in dynamics simulations of bilayers of 14–2–14. In this case, the N–N vectors are tilted up to  $33^\circ$  from the surface of the bilayer.<sup>28</sup> This type of phenomenon was also observed with monolayers of fatty acids.<sup>29</sup> In such systems, carboxylate groups are dispersed perpendicular to the monolayer in order to lower the charge density.

In summary, it can be suggested that the N–N azimuth angle is controlled by the competition between charge repulsion between the headgroups and steric repulsion between hydrophobic chains. This orientation may arise from a collective behavior (molecules may not orient independently from each other) or from an individual orientational preference of each molecule.

From dichroic signals of PM-IRLD measurements, a preferred orientation of water molecules was observed in

the case of micelles formed with 12–2–12 and 8–2–16. The negative band at  $1650\text{ cm}^{-1}$  indeed indicates that the bending of the water molecules, which is parallel to their dipole moment, defines an angle between  $54.7^\circ$  and  $125.3^\circ$  with the micellar axis. In parallel, molecular dynamics simulations show that the dipole moments of water molecules are preferentially oriented in a plane perpendicular to the micelle (Figure 8). The excellent agreement between these unexpected results is remarkable. To the best of our knowledge, such an induction of water molecule orientation by micellar structures has not yet been reported.

Taking a mean value of the orientation of the water dipoles perpendicular to the micellar axis, two cylindrical distributions may be proposed ( $\alpha = 90^\circ$  in Figure 1c): the dipole may either be parallel to the cylinder surface and perpendicular to the cylinder axis and the cylinder surface. The first configuration is less likely, since it would be energetically very similar to the configuration where dipoles are oriented parallel to the cylinder axis as well as the cylinder surface, which should result in a positive PM-IRLD band that may overall cancel the dichroism. More likely, water molecules are pointing radially to the cylinder.

As shown below, it is possible to roughly estimate the thickness of the oriented water layer from the spectroscopic data. In the following, the thickness is calculated for a 240 mM solution of 8–2–16. From the peak maximum at  $1650\text{ cm}^{-1}$  on the transmission spectra (not shown), the absorbance of the water bending band can be deduced to be about 0.5. From the refractive index of water, the actual thickness of water in the sample was calculated to be 4.5  $\mu\text{m}$ . The absorbance of the water bending band is proportional to the extinction coefficient of water,

$$A = ak_l \quad (4)$$

where  $A$  is the absorbance of water,  $k$  is the extinction coefficient,  $l$  is the thickness of water, and  $a$  is a proportionality coefficient. Therefore, for the nonoriented water,

$$0.5 = ak \times 4.5(\mu\text{m}) \quad (5)$$

When water is not oriented,  $k$  is expressed as

$$k = k_{\text{nonorient}} = \frac{1}{3}(k_x + k_y + k_z) \quad (6)$$

As discussed previously, the negative dichroic signal of water molecules indicates an orientation perpendicular to the cylinder axis (Figure 18). If among the three orthogonal directions  $xyz$ , we choose  $x$  to be parallel to the incident beam and  $z$  parallel to the cylinder axis, and if we consider from the simplified model that all water molecules are in the  $xy$  plane, then the extinction coefficient of oriented water molecules can be written as

$$k = \frac{1}{3}(k_{0x} + k_{0y} + 0) = \frac{2}{3}k_{0x} = \frac{2}{3}k_{0y} \quad (7)$$

$\Delta A$  for the bending band of water at  $1650\text{ cm}^{-1}$  is about 0.025 for the 8–2–16 240 mM sample as described above. We first calculate the thickness of orientated water molecules assuming 100% of the molecules are oriented in this domain.

$$0.025 = ak_{0x}l_{\text{orient}} \quad (8)$$

(28) Manuscript in preparation.

(29) Kmetko, J.; Datta, A.; Evmenenko, G.; Dutta, P. *J. Phys. Chem. B* **2001**, *105*, 10818.

From eqs 5–8, the total thickness of oriented water can be calculated as

$$l_{\text{orient}} = \frac{2}{3} \times 4.5 \times \frac{0.025}{0.5} = 0.15 \mu\text{m} \quad (9)$$

We can then estimate the thickness of micelles crossed by the IR beam from the concentration of the surfactant. The concentration is about 15% v/v; therefore the total thickness of micelles crossed by the beam is  $4.5/(1 - 0.15) \times 0.15 = 0.794 \mu\text{m}$ . Since micelles have a cylindrical shape, each micelle of ca. 25 Å in radius can be approximated to have a mean thickness of  $\pi r^2/2r \sim 40 \text{ Å}$ ; therefore the IR beam crosses about  $794/4$  or 200 micelles. Then, from eq 9, the thickness of the oriented water layer on each side of a micelle is

$$x = 0.15 \mu\text{m}/(200 \times 2) = 3.75 \text{ Å}$$

This value is compared with the thickness of bound water molecules (5–7 Å) calculated from the dynamics simulation. It should be corrected for the fact that oriented water molecules are certainly not all perfectly perpendicular to the cylinder axis.

Finally, the PM-IRLD data of micelles of the fluorinated gemini surfactants are quite intriguing. The aggregates' morphologies are similar to those of their hydrogenated homologues, and the positive dichroic signals indicating either preferred 45° orientation or random orientation with cylindrical symmetry for the CF<sub>2</sub> groups are observed as for the CH<sub>2</sub> chains. However, in this case no dichroic signal is observed for water molecules. Instead, a small negative component assigned to the carboxylates of tartrate indicates an orientation of the counterions around the micelles. Either the water molecules are not so tightly bound, or their orientations are not well-defined in the presence of the tartrate ions.

### Conclusion

We have investigated the molecular organization of cationic hydrogenated and fluorinated gemini surfactants in cylindrical micellar structures. PM-IRLD was performed on the solution of shear-aligned cylindrical mi-

celles. The positive dichroic signals of the stretching vibration of CH<sub>2</sub> and CF<sub>2</sub> of the hydrophobic chains indicate that if the chains have a preferred orientation, the average direction of the symmetric vibration of the CH<sub>2</sub> or CF<sub>2</sub> groups of the alkyl chains is ca. 45° from the cylinder axis. From such a value, one can estimate that the N–N direction of the gemini molecules is oriented either at ca. 35° or at ca. 55°. However, from the model that we have constructed to analyze the PM-IRLD signals, there is a subsisting ambiguity since positive dichroic signals do not allow us to determine whether molecules organized with cylindrical symmetry have a preferred direction along the cylinder axis or whether they are randomly oriented. On the other hand, the water molecules around the cylindrical micelles of gemini molecules having bromide counterions show negative dichroic signals, clearly indicating an orientation of water molecules perpendicular to the cylinder axis within a layer of ca. 4 Å. Such water molecule orientation was not observed with cylindrical micelles of fluorinated gemini surfactants having tartrate counterions.

In parallel, molecular dynamics simulations were performed on a cylindrical micelle. The H–H vectors of the CH<sub>2</sub> groups in the alkyl chains show an orientation at ca. 45° and that of the N–N vectors is between 30 and 60°, which supports an interpretation of the PM-IRLD data based on preferred molecular orientation. It was also calculated that a majority of water molecules in the simulation box are oriented perpendicular to the cylinder axis. From the diffusion constant of water molecules, the thickness of oriented water was estimated to be ca. 6 Å. Such observations corroborate our IR measurements very well.

The fact that N–N vectors are oriented at such angles from the cylinder axis can be interpreted as the result of a competition between charge repulsions between head-groups and steric repulsions between hydrophobic tails.

**Acknowledgment.** This work was supported by the CNRS, the University of Bordeaux I, the Ecole Polytechnique, and the Aquitaine region. The authors thank Gilles Moreau for the Fortran program used for analyzing the angles projected in cylindrical symmetry.

LA026051M